Quantitative Biology
https://doi.org/10.15302/J-QB-022-0281

RESEARCH ARTICLE

Physics-informed machine learning for the COVID-19 pandemic: Adherence to social distancing and short-term predictions for eight countries

Georgios D. Barmparis[1,†,*], Giorgos P. Tsironis[1,†,*]

[1] Institute of Theoretical and Computational Physics and Department of Physics, University of Crete, Heraklion 71003, Greece
* Correspondence: barmparis@physics.uoc.gr; gts@physics.uoc.gr

Received April 9, 2021; Revised May 20, 2021; Accepted June 15, 2021

***Background*: The analysis of COVID-19 infection data through the eye of Physics-inspired Artificial Intelligence leads to a clearer understanding of the infection dynamics and assists in predicting future evolution. The spreading of the pandemic during the first half of 2020 was curtailed to a larger or lesser extent through social distancing measures imposed by most countries. In the context of the standard Susceptible-Infected-Recovered (SIR) model, changes in social distancing enter through time-dependent infection rates.**
***Methods*: In this work we use machine learning and the infection dynamical equations of SIR to extract from the infection data the degree of social distancing and, through it, assess the effectiveness of the imposed measures.**
***Results*: Quantitative machine learning analysis is applied to eight countries with infection data from the first viral wave. We find as two extremes Greece and USA where the measures were successful and unsuccessful, respectively, in limiting spreading. This physics-based neural network approach is employed to the second wave of the infection, and by training the network with the new data, we extract the time-dependent infection rate and make short-term predictions with a week-long or even longer horizon. This algorithmic approach is applied to all eight countries with good short-term results. The data for Greece is analyzed in more detail from August to December 2020.**
***Conclusions*: The model captures the essential spreading dynamics and gives useful projections for the spreading, both in the short-term but also for a more intermediate horizon, based on specific social distancing measures that are extracted directly from the data.**

Keywords: COVID-19; physics-informed machine learning; SIR; time-dependent infection rate; short-term predictions

Author summary: This work combines machine learning techniques with mathematical models known in epidemiology, enabling the extraction of COVID-19 infection information in different countries. This approach controls the data-driven information and shows how various measures and practices in each country are directly reflected in the infection data. The use of machine learning, especially neural networks, allows the extraction of the time-dependent infection rate that drives the evolution of the pandemic in each country. Knowledge of the time-dependent infection rate allows short-term predictions with a week-long or even longer horizon.

INTRODUCTION

The COVID-19 pandemic started in December 2019 and subsequently spread fast in the world. After an initial "hesitant" approach, most countries essentially adopted social distancing rules that originated in China. Several countries delayed the imposition of measures and, as a result, saw large numbers of infected persons and

[†] These authors contributed equally to this work.

deaths. Other countries acted very swiftly and managed to control the infected numbers and especially the mode of spreading. There was an initial discussion related to "herd immunity" that was in part attempted by some countries, but soon the basic global approach was that introduced by China, *i.e*. social distancing. However, the degree and swiftness of social distancing were different in each country; in Italy and Spain, for instance, there was an initial delay while Greece acted very quickly and with strong measures. The control of the epidemic has been the main subject in many studies, and several kinds of epidemic models have been used to address the question of how control measures could limit the pandemic growth. Hufnagel *et al.* [1] introduced a stochastic model where stochastic local infection dynamics among individuals were combined with stochastic transport in a worldwide network, taking into account national and international civil aviation traffic. Different control strategies were analyzed concluding that a quick and focused reaction is essential to inhibiting the global spread of epidemics. Baker *et al.* [2] used a climate-dependent epidemic model to simulate the SARS-CoV-2 pandemic by probing different scenarios based on known coronavirus biology. They found that without effective control measures, strong outbreaks are likely in more humid climates and summer weather will not substantially limit pandemic growth. Qui *et al.* [3] used an empirical model to quantify the impact of social and economic factors on the transmission of coronavirus disease in China. Ardabili *et al.* [4, 5] presented a comparative analysis of machine learning and soft computing models to predict the COVID-19 outbreak as an alternative to Susceptible–Infected–Recovered (SIR) and Susceptible-Exposed-Infectious-Removed (SEIR) models. Pinter *et al.* [6] proposed hybrid machine learning methods of adaptive network-based fuzzy inference system and multi-layered perceptron-imperialist competitive algorithm to predict time series of infected individuals and mortality rates. Ramon Gomes da Silva *et al.* [7] used several machine learning methods including Bayesian regression neural network, cubist regression, k-nearest neighbors, quantile random forest, and support vector regression, coupled with climatic exogenous variables to forecast the COVID-19 cases in five Brazilian and American states. More sophisticated SIR-type models were also used in predicting the evolution of the COVID-19 pandemic. Zhao and Chen [8] used a Susceptible, Un-quarantined infected, Quarantined infected, Confirmed infected (SUQC) model for modeling the epidemic dynamics and control of COVID-19 in China. A spatio-temporal SEIR-type model including categories for N age and sex groups in M different spatial locations was proposed by Albani *et al.* [9] to simulate and monitor the (COVID-19) epidemic evolution in New York City. Lytras *et al.* [10] used a modified Bayesian SEIR model for estimating the ascertainment rate of SARS-CoV-2 infection in Wuhan, China. Although ultimately the effectiveness of any measure is reflected in the number of deaths, in this work, we use the more error-prone infection data for a number of reasons. The infection data are representative of the dynamics of the disease at the country level, even though they clearly depend on the number of tests performed. At the initial phase, the test availability was limited, and thus it was used on a need to be the basis and, as a result, targeted more closely individuals with symptoms. Additionally, since the COVID-19 pandemic affects people of older ages primarily, the death data are strongly age biased and thus do not reflect the true dynamics of the spreading that leads to these deaths.

In an earlier publication, the first version of which appeared in the arXiv on March 31, 2020, *i.e*., right in the middle of the pandemic, we used a Gaussian hypothesis for the spreading of the disease and number of infected persons and predicted the spreading and the horizon of the first wave [11]. We showed that this specific functional dependence originated from the imposed measures and, in particular, from an approximately linear reduction in the infection rate $\alpha(t)$ as a result of imposed measures. This hypothesis proved to have two-fold usefulness: On one hand, it gave a good prediction for the horizon of the epidemic in countries like Greece, Italy, and Spain while the measures were in effect. On the other hand, for countries such as the US and UK where measures either did not enforce in full strength or were not applied fast enough, the prediction of the model based on the Gaussian hypothesis was rather poor. Although this was expected, it nevertheless gives a very good way to assess now, *i.e*. after the fact, how efficient were the measures in these and other countries. This may be done by evaluating from the real data an effective number that gives a degree of the harshness of imposed measures, adequate timing, etc. This number, denoted by σ, is the slope of the assumed linear dependent decay of the infection rate coefficient. Large σ means that the effective measures where drastic and applied on time while, in the other extreme, $\sigma \approx 0$ signifies the practical absence of measures.

The present study rests heavily on Physics with Artificial Intelligence (PhAI) where physics modeling with machine learning are employed in a coordinated way. Specifically, here we start with an SIR model [12] and use analytics in order to derive a differential equation of the infection rate $\alpha(t)$; this equation contains the information on the individual infection percentage in the population. We then take the data for the country's infected population and estimate the infection rate $\alpha(t)$.

This step is done by using Machine Learning (ML) techniques and, in particular, by using physics-informed neural networks (PINN). We pre-train the latter on simulated SIR data and subsequently train it on each country's reported infected data. Instead of assessing a general $\alpha(t)$ curve, we assume a linear functional dependence explicitly; its slope σ is the result of the ML procedure we apply. Once the infection rate is known, we validate the resulting SIR model to the country's data and then vary σ to see the changes in the epidemic. This procedure gives a clear picture of both of the effective measures in each country but also their efficiency.

The assumption of linear decay in $\alpha(t)$ with slope σ is tantamount to an effective linearization to the actual infection rates. Clearly, other, more complex forms may be assumed. We find that this simple form can efficiently capture the nature of the phenomenon and give a simple quantitative estimate of the imposed measures. The values of the slope σ are obtained directly through ML and, thus, in a sense, are directly derived from the infection data. Thus, we may link each infection curve with an effective decay slope σ that denotes the overall control that the measures exercise on the infection phenomenon. Since the approach is fundamentally data-driven, the knowledge of a particular slope gives a handling on the possible measures exercised. Furthermore, once the PINN we develop works well, we may use it to make predictions. Specifically, we use data from the second phase of the spreading, that we assume starts after the initial decline in the infection, train the network with this data and make short-term predictions for the current period.

MATHEMATICAL MODELING

The simple Susceptible-Infected-Removed (SIR) infection model is very powerful in determining qualitative but also quantitative aspects of the COVID-19 pandemic [12]. The basic equations are

$$\frac{\mathrm{d}S}{\mathrm{d}t} = -\alpha SI, \tag{1}$$

$$\frac{\mathrm{d}I}{\mathrm{d}t} = \alpha SI - \mu I, \tag{2}$$

where $S \equiv S(t)$, $I \equiv I(t)$ are the percentage of susceptible and infected individuals respectively and the infection and removal rates $\alpha \equiv \alpha(t)$, $\mu = \mu(t)$ respectively are functions of time in general. We introduce the variable $q(t)$ through the ansatz:

$$I(t) = e^{q(t) - \int_0^t \mu(t')dt'}. \tag{3}$$

Upon substitution to the set of Eqs. (1,2) we obtain

$$\dot{S} = -\alpha e^{q-\nu} S, \tag{4}$$

$$\dot{q} = \alpha S, \tag{5}$$

$$\nu \equiv \nu(t) = \int_0^t \mu(t')dt'. \tag{6}$$

Using Eqs. (4,5) we obtain a closed equation for q, *i.e.*,

$$\ddot{q} = -\left(\alpha e^{q-\nu} - \frac{\dot{\alpha}}{\alpha}\right)\dot{q} \tag{7}$$

Equation (7) is a unique second order equation that fully captures the dynamics of the SIR infection model. While it is highly nonlinear, it is nevertheless quite useful in determining the infection dynamics since it is general and contains the arbitrary time dependence of both the infection and removal rates. It will be used subsequently in the application of ML techniques to the COVID-19 infection data. In the case of constant infection and removal rates it can be solved exactly (in Methods section).

In order to work with a time dependent infection rate $\alpha(t)$, we start with the general Eq. (7) and we assume for simplicity that the recovery rate $\mu(t) \equiv \mu$ is a constant; in this case the expression of Eq. (7) simplifies to $\nu = \mu t$ and thus $I(t) = exp[q(t) - \mu t]$. We may start from Eq. (7) and obtain a first order equation for the infection rate (see Eq. (27) in Methods). This is useful since we are interested in the inverse problem of finding the infection rate from the data. The specific form of $\alpha(t)$ determines the infection evolution. We know, for instance, that a monotonic linear drop in the infection rate, as for instance introduced by gradual social distancing measures results in an approximately Gaussian evolution [11].

For the analysis of the first wave we will consider the case where the infected population behaves similar to a Gaussian function [11]. In the Gaussian exponent we will keep a linear time-term in addition to the quadratic one; this new term is useful since it provides some time asymmetry; we thus take

$$q(t) = \beta t^2 + \gamma t. \tag{8}$$

Some algebra (details in Methods) leads to the analytical expression

$$\alpha(t) = (2\beta t + \gamma)\left[\alpha(0)\gamma + \frac{2\beta}{2\beta t + \gamma} - (\gamma - \mu)e^{\beta t^2 + (\gamma - \mu)t}\right]. \tag{9}$$

We note that the dominant term is that of linear decay since at longer times and $\beta < 0$ the Gaussian term in Eq. (9) essentially disappears while the exponential term also decays when $\mu > \gamma$. In general, of course, the functional dependence of $\alpha(t)$ is more complex and in cases with strong asymmetry introduced by γ we have

distinctly nonlinear decay. We observe thus how significant is the precise functional form of the time dependent infection rates for the general evolution of the SIR modeling of the infection phenomenon. This general shape of $\alpha(t)$ will be used in what follows.

Machine learning application

We approximate each country's daily reported cases using a deep neural network containing one input node, five hidden layers of 100 nodes with a "sigmoid" activation function, and one output node. Initially, we use simulated SIR data and an arbitrary linear function for $\alpha(t)$ with a constant value for μ, to train the model. The model is trained, using a custom training loop, by minimizing the mean squared error loss on the data, MSE_D:

$$MSE_D = \frac{1}{N_D}\sum_{i=1}^{N_D}|x_i - \tilde{x}_i|^2, \tag{10}$$

where $\{x_i, \tilde{x}_i\}_{i=1}^{N_D}$ denote the set of the reported, $x_i = ln(I_i)$, and corresponding predicted cases, $\tilde{x}_i = model(t_i)$ and the mean squared error loss defined by Eq. (7) with $\alpha = \alpha(t) = \sigma_0 + \sigma t$, $\nu = \mu t$ (*i.e.*, μ = constant), and $\tilde{x} = q(t) - \mu t$, MSE_{SIR}:

$$MSE_{SIR} = \frac{1}{N_{SIR}}\sum_{j=1}^{N_{SIR}}|f(t_j, \tilde{x}_j, \dot{\tilde{x}}_j, \ddot{\tilde{x}}_j, \sigma_0, \sigma, \mu)|^2, \tag{11}$$

where,

$$f(t_j, \tilde{x}_j, \dot{\tilde{x}}_j, \ddot{\tilde{x}}_j, \sigma_0, \sigma, \mu) = \ddot{\tilde{x}}_j + \left(\alpha_j e^{\tilde{x}_j} - \frac{\dot{\alpha}_j}{\alpha_j}\right)(\dot{\tilde{x}}_j + \mu) = 0. \tag{12}$$

Then for each of the countries into consideration, we load the real data and smooth it using a seven time-steps moving average. We then scale the data using Min-Max normalization. We load the pre-trained model and allow all its weights to be tuned by minimizing again both the MSE_D and MSE_{SIR} loss functions on the country's data, getting at the same time the optimal values for $\alpha(t)$ and μ for the given country. The pre-trained model is used to accelerate each country's training process. The training process of each country stops using early stopping with a horizon of 100 epochs. The machine learning algorithms were implemented in Python using TensorFlow [13]/Keras [14] and the ADAM [15] optimizer. The data used in this study are published online at OurWorldInData.org [16] and the code is available on GitHub [17].

A graphical summary of the procedures used in this work and how the results and predictions are obtained is shown in Fig. 1.

Results

The ML model with analytical results will be used both for the analysis of the first wave of the infections, but also for making short-term predictions for the second wave. In the former case we assess the effectiveness of measures while in the second we make useful predictions.

Feature extraction through pre-trained, physics informed neural networks

The exact mathematical analysis of the SIR model is important for the analysis of the data through ML techniques. The COVID-19 "first wave" started at different times in various countries and had a completely different evolution. In countries where very restrictive measures similar to those of China were imposed an effective spreading control swiftly was accomplished. Other countries that either delayed or imposed partial or essentially no measures saw larger numbers in the infected population and slower decay in the infected numbers. Here we make no judgment as to whether measures were "good" or "bad", but we simply want to be able to extract the presence of the measures from the dynamics of the infected population. Specifically, we would like to see what is the imprint of social distancing in the distribution of the infected population across the eight model countries we follow. To accomplish this, we use a strategy that utilizes methods from artificial intelligence and in particular ML. The basic assumption in our approach is that the SIR model can capture the essentials of the epidemic in each country. A direct consequence of this assumption is that we can use simulated data from the SIR model to pre-train the specific neural networks we use for each country.

The application of ML techniques to data often suffers from the fact that data are considered "pure" with no connection to a specific phenomenon. A remedy towards introducing specificity is through the use of physics-informed techniques where the ML processes, typically those involving artificial neural networks (ANN), are restricted imposed by physical laws in mathematical form [18]. In the specific problem, the SIR equations play this role and put strict bounds to the ANN used for simulating the phenomenon. Once we have a physics-informed network that is trained on the infected data of the specific country, we may use it to extract the presence and persistence of the social distancing measures typified through the function $\alpha(t)$. Since the ANN finds a general decay and also given the discussion in the previous section, we posit a linear dependence in the form $\alpha(t) = \sigma_0 + \sigma t$, where the

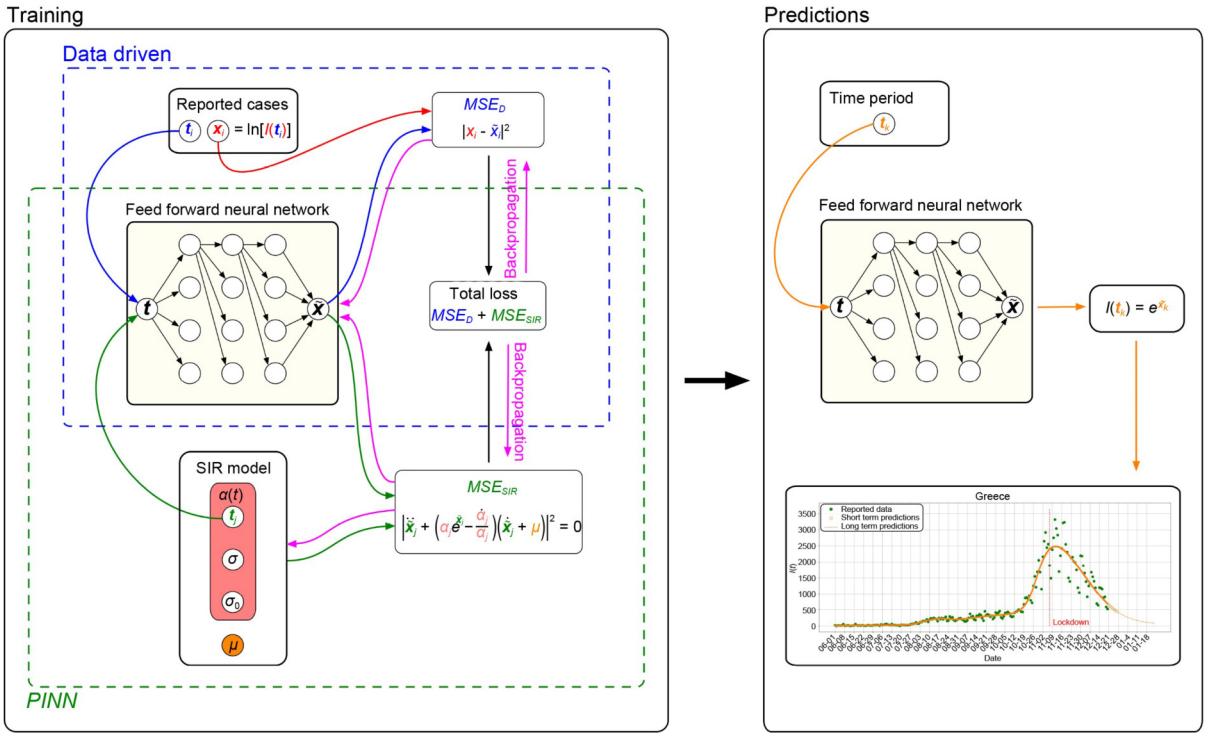

Figure 1. A Graphical summary of the methods and results of this work.

intercept σ_0 and the slope σ are determined through the ANN. The slope σ, in particular, is a parameter with an important physical significance, since it estimates within the linearized model the degree of efficiency of social distancing. In other words, a large value in σ describes in an average way a country that followed through the first wave strict social distancing measures while, on the contrary, small values in the slope denote much looser adherence to measures. We note that these measures are not necessarily the externally imposed ones but also include the self-imposed measures.

Having extracted the optimal $\alpha(t)$ as well as μ for each country, we use them to solve the SIR model, Eqs. (1, 2). The solution is then fitted to the country's real data using the initial conditions (I_0, S_0) as fitting parameters. The total number of the predicted cases during the "first wave" period of each country, including the relative error to the corresponding total number of reported cases and the total number of cases obtained by varying $\alpha(t)$ by ± 10%, is presented in the Table 1. A plot of the results for each country is shown in Fig. 2.

Short-term predictions

The arsenal of PhAI was used in the previous section in order to extract dynamical parameters such as the time-dependent infection as well as the removal rates from the documented infection data. The procedure through SIR pre-training proved to be quite efficient and gave a hierarchy of $\alpha(t)$ for different countries for the initial period of the infection. It is both tempting as well as challenging to apply this procedure to the present phase of the COVID-19 pandemic and attempt to make future predictions. In the process of future point evaluations, our procedure needs to satisfy two constraints; one is the overall mean square minimization that reduces the overall error. The second is the one imposed by physics, *i.e.*, it must follow the SIR model. In order to accomplish the latter, the procedure needs to know the functional of $\alpha(t)$ as well as the value of μ at the future points. We provide this information through the extrapolation of the values from the previous times. Once these values are known, the SIR dynamics is warrantied and provides the second, physics derive constraint.

In Fig. 3 we show the evolution of the current phase of the pandemic as well as the prediction obtained for a horizon of one week. In preparing these results, we used the available COVID-19 data, starting precisely where the first phase ended and used it up to one week before end dates for all eight countries for PINN training. Subsequently, we used the network for prediction and compared the results with the existing data. We note that the network's short-term predictive power is quite good on average in most countries.

Table 1 Left: Total number of reported cases during the "first wave" for each country and the corresponding predicted cases and percentage error obtained from our model, including the predictions with ± 10% variation of $\alpha(t)$. Right: A bar plot of the slope $-\sigma$ of each country signifying the degree of adherence to measures. The higher the bar, the more reduced is the transmission rate due to the control measures.

Country	Total cases		Error (%)	$\alpha(t)+10\%$ (% Difference)	$\alpha(t)-10\%$ (% Difference)	R^2
	Reported	Predicted				
USA	1961185	1945830	−0.8	1793214 (−7.8)	2063029 (6.0)	0.944
Italy	240961	275667	14.4	259349 (−5.9)	284978 (3.4)	0.863
Spain	245938	280859	14.2	249833 (−11.1)	298190 (6.2)	0.791
UK	286141	312211	9.1	217528 (−30.3)	382591 (22.5)	0.872
Germany	186839	215563	9.5	182532 (−15.3)	233021 (8.1)	0.776
The Netherlands	50412	55040	9.2	52524 (−4.6)	56583 (2.8)	0.837
France	149668	163580	9.3	117539 (−28.2)	187154 (14.4)	0.702
Greece	2967	3014	1.6	2794 (−7.3)	3155 (4.7)	0.540

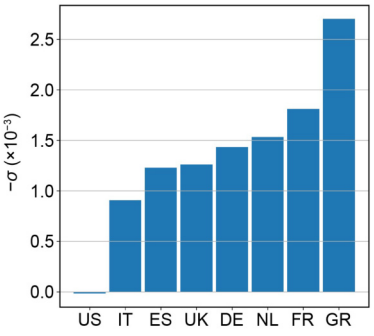

DISCUSSION

The spreading of COVID-19 has generated a wave of illness and death worldwide, accompanied by a severe disruption in financial, educational, commercial activities, global travel etc [1, 21−24]. During the first phase of the spreading, there were different approaches to the measures to be taken to slow it down. Different countries reacted in different ways, and, as a result, the epidemic dynamics proceeded differently. The infection curves were different and dependent strongly both on the imposed social distancing measures and the adoption of responsible practices from individuals. One important aspect of the pandemic is to find ways to assess the degree to which the social distancing measures where followed. It is not trivial to extract this information from the data since the infection dynamics are directly related to the imposed social distancing measures. Furthermore, this cannot be done in a completely data-driven way, and thus assumptions about both the model and the way measures are imposed are important.

In the present work, we followed an early attempt [11] and used the publicly available infection data to assess the effectiveness and adherence to social distancing in different countries; in doing this analysis, we assumed that the mathematical model underlying the infection dynamics is the simplest SIR model. Before using the arsenal of ML we tackled the model analytically and produced two basic results; the first one is a general analytical solution for the model obtained through a specific exponential ansatz. The second, also dependent on this ansatz, is a differential equation for the function $\alpha(t)$ that describes the time dependent nature of the infection rate. The latter depends strictly on the imposed social distancing measures as well as the practices of the individuals. We pointed out, as also in reference [11], that a linear drop in the infection rate leads to an approximate Gaussian functional dependence in the infected population. The specifics of this functional form depends both on the form as well as values of $\alpha(t)$ but also on the removal rate μ.

In order to extract the time-dependent infection rate from the data, we used physics-informed neural networks, *i.e.*, a machine learning method that uses input from the actual model assumed, viz. SIR. This input, together with the real infection data from each country we considered, led to a prediction of the assumed linear in time infection rate. The data derived slope σ signifies the adherence of each country to social distancing. In Greece, for instance, the slope is large in absolute value, designating strong application of the imposed measures by the individuals. In the other extreme, we find the USA with a practically zero slope, demonstrating that the measures taken had low efficiency. The other six countries we analyzed fall in intermediate locations between these two extremes. Application to the SIR model of each country, an alternative infection rate that differs by a few percent (±10%) in total from the one obtained through ML gives an estimate of how dependent the infection is on the applied measures. We find that this variation, while it affects the early SIR fast rise strongly, results in quite a different infection decay and horizon in countries like the UK.

Once we know how the PINN behaves with the data for the initial period of the infection, we may use it for the second phase. We consider that the latter starts from the end of the initial period and reaches the present day. Thus, we use country infection data during this period except for the last week to train the network and subsequently make predictions for the last week and compare it with real data. We find that while the short-term predictive power of PINN is good, it has large deviations in countries where the data appear to have a rather stochastic character.

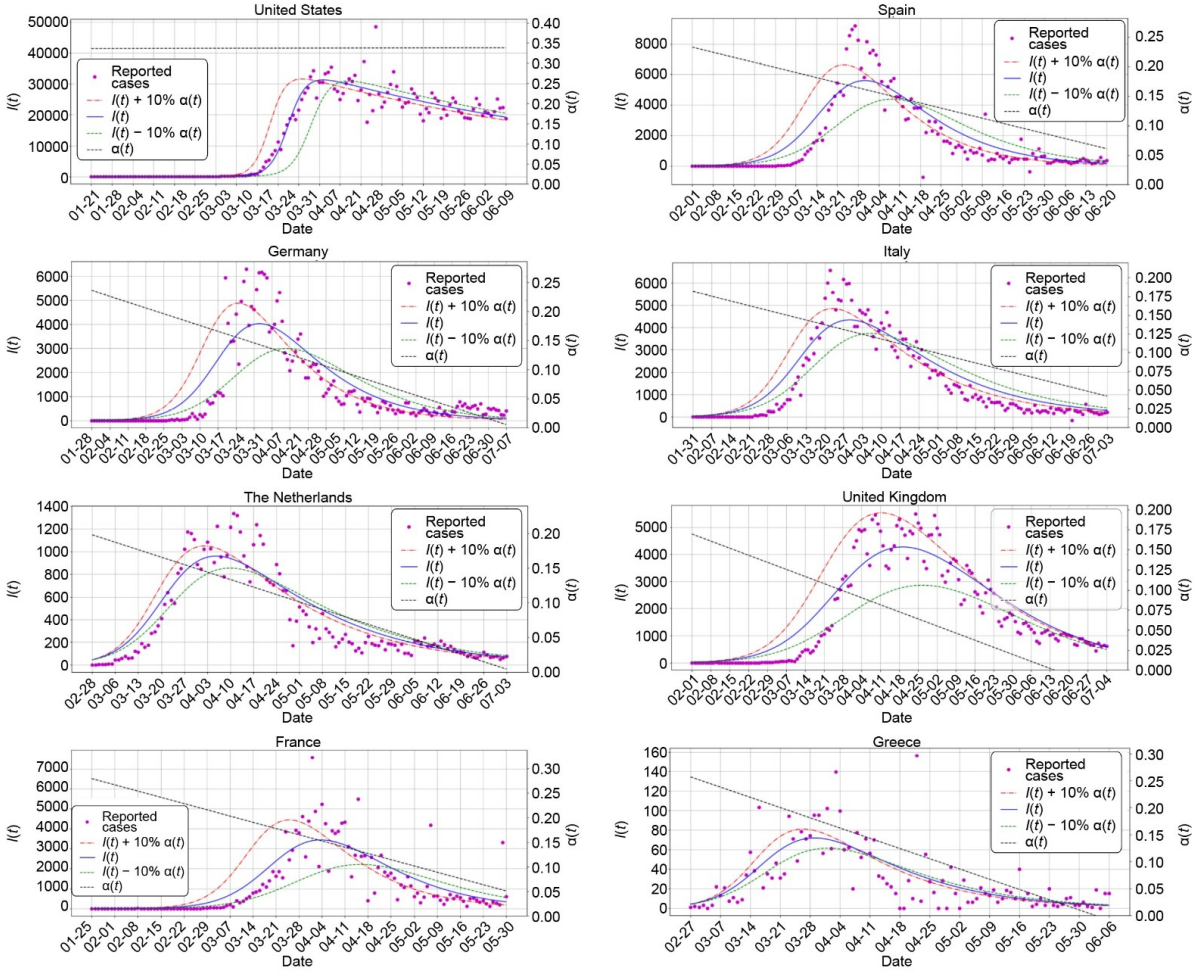

Figure 2. Country level predicted infections, $I(t)$, for the extracted $\alpha(t)$ of each country. Magenta dots represent the reported cases of each country. Red, dashed and dotted line, blue solid and green dashed line represent the infections with +10%, no change, −10% to the infection rate $\alpha(t)$, respectively. Black dashed line represents the extracted infection rate of each country.

We applied these methods to the case of Greece for the period since the original posting of the preprint to the arXiv (August 18, 2020) until December 18, 2020, *i.e.*, for a period of four months. We made predictions every Friday evening with a horizon of one week. In Greece, there was a lockdown imposed on November 7 2020. In Fig. 4 we present the comparison of the weekly PINN model predictions to the actual reported data after each prediction period, including the weekly total reported and predicted cases and the relative error. Additionally, we show longer prediction horizons based on data in different periods of the pandemic evolution. We observe that the model is quite adoptive to the data behavior, and it gives a quite good short-term average prediction, when the infection rate does not change rapidly (relative error 0.3% to 9.2%). It also demonstrates the degree of effectiveness of the measures. On the contrary, the model does not follow the pandemic's evolution when the infection rate changes very rapidly, either increasing, as during the week between October 19 and October 26 (relative error −33.8%) or decreasing, *i.e.*, immediately after the lockdown on November 7 (relative error 31.7% to 55.3%). The relatively increased error is due to the sharp imposition of measures exactly that week. This clearly changes abruptly the infection rate and the model captures this change in the next predictive period.

The basic conclusion of this work is that the use of physics-informed ML may enable the extraction of COVID-19 infection information in different countries, show how different measures and practices are directly reflected in the data and ultimately make predictions. The use of physics in machine learning gives specificity to the data, but, on the other hand, is restricted and some times limited to inserted physics knowledge. The present approach assumes a well-mixed, essentially uniform

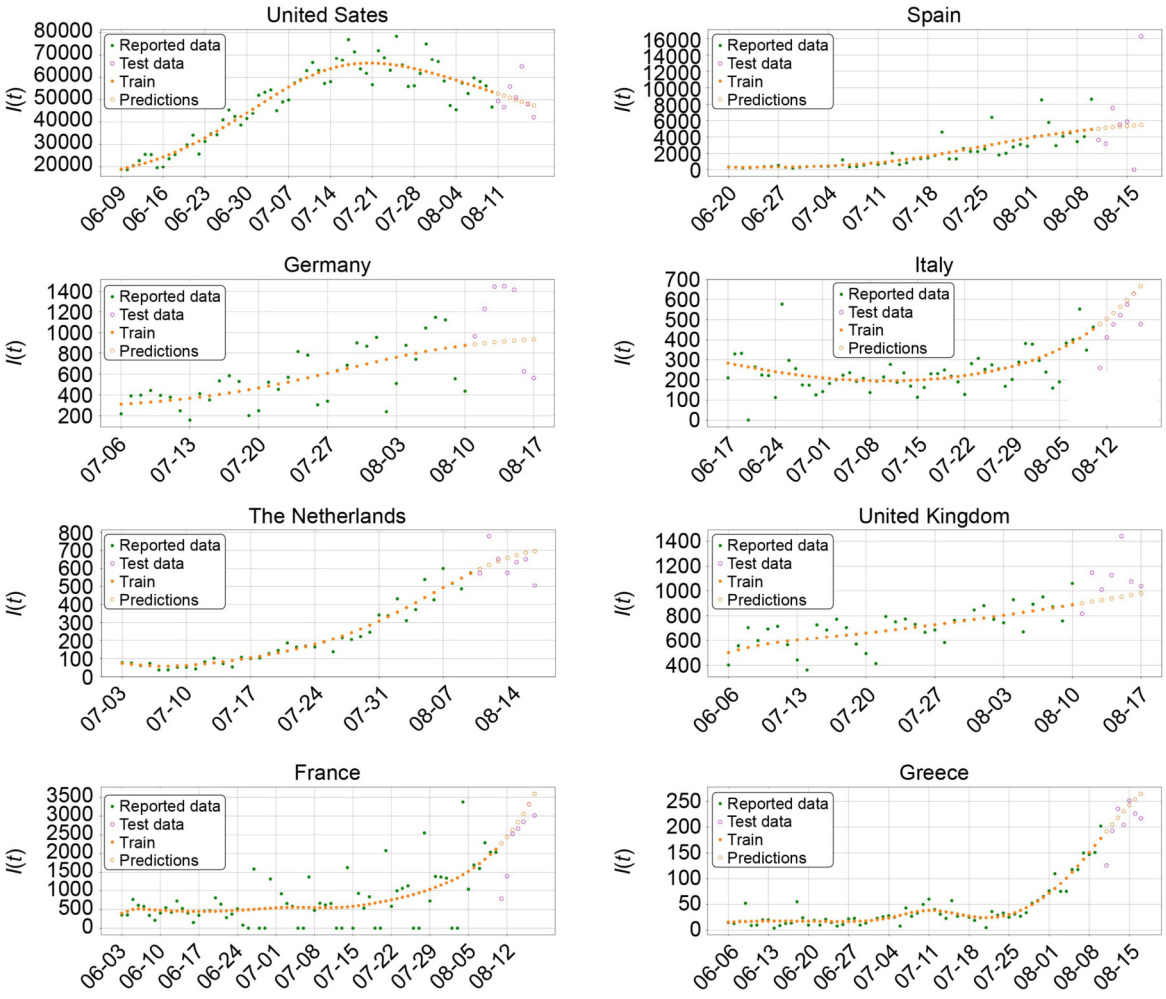

Figure 3. We use data of the second phase of COVID-19 spreading except for the last week, we train the network and predict the evolution during the last week. The percentage error in the total number of predicted cases of each country found to be −1.75% for the US, −35.4% for ES, −16.7% for DE, 18.6% for IT, 4.5% for NL, −14.2% for the UK, 31.6% for FR and 10.5% for GR.

country, an assumption that is introduced through the use of the SIR model. However, countries have regions, and each region may behave differently for geographical, environmental, cultural, as well as population reasons. If regional data is available, one can go one step further and introduce spatial in addition to temporal distribution in the infection and from this be able to obtain more accurate results and predictions. We believe the methodology used in this work may be extended in this more realistic case and provide a more direct approach to local dynamics and the effectiveness of imposed measures at a local level.

Limitations

The present approach depends on the SIR model as well as the fact that naturally we do not know the time dependent infection rate $\alpha(t)$ during the prediction period. As a result we assume that during the prediction period the infection rate is that of the previous appropriate time segment (or at least it does not change rapidly). One could envision using other epidemiological models for the physics-informed ML or even more sophisticated neural network architectures than the feed forward networks (FFN), *i.e.*, the recurrent neural networks, like the long-short term memory models (LSTM), as well as make other projections for the rate $\alpha(t)$. These could lead to improved prediction accuracy.

METHODS

Time-independent infection rates

For the simpler case of constant α and μ, Eq. (7) becomes

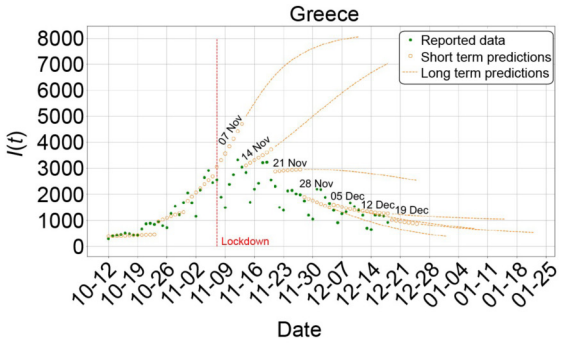

Week	Total cases		Error (%)
	Reported	Predicted	
10/10−10/17	2678	2782	3.9
10/17−10/24	4607	3050	−33.8
10/24−10/31	8139	8002	−1.7
10/31−11/07	15058	15591	3.5
11/07−11/14	17421	27049	55.3
11/14−11/21	18137	23885	31.7
11/21−11/28	13475	20412	51.5
11/28−12/05	11898	11865	−0.3
12/05−12/12	9463	10330	9.2
12/12−12/19	6936	9124	31.5

Figure 4. Left: PINN-ML model applied to Greece infection data (green filled circles) for a period of approximately four months. The predictions are weekly (open orange circles) or longer term (dashed lines). The trend of the infection is generally captured by the predictions. The imposition of the lockdown changes dramatically the dynamics of $\alpha(t)$ and this is reflected immediately in the short-term predictions. The intermediate term predictions demonstrate clearly the effectiveness of the lockdown and predict the observed show decay of the spreading. The dates on the graphs inform on the date the intermediate prediction was evaluated. Right: Weekly total reported and predicted cases, and the relative error (negative values mean underestimated prediction by the model, positive values, overestimated prediction by the model).

$$\ddot{q} = -\alpha e^{q-\mu t}\dot{q}. \tag{13}$$

Introducing the transformation $x = q - \mu t$ we turn Eq. (13) into the following form:

$$\ddot{x} + \alpha e^{x}\dot{x} + \alpha\mu e^{x} = 0. \tag{14}$$

The new initial conditions are $x(0) = \ln I(0)$ and $\dot{x}(0) = aS(0) - \mu$. The Eq. (14) is a Lienard Equation that can be turned into an Abel equation through the introduction of the transformation [25]

$$y(x) = \dot{x}. \tag{15}$$

We obtain the following Abel equation of the second kind:

$$yy_x = f_1(x)y + f_0(x), \tag{16}$$

$$f_1(x) = -\alpha e^{x},\ f_0(x) = -\alpha\mu e^{x}. \tag{17}$$

We introduce further the variable ξ as follows

$$\xi = \int f_1(x)dx = -\alpha e^{x}. \tag{18}$$

Since $y_x = y_\xi f_1(x)$, Eq. (16) becomes

$$yy_\xi = y + \mu. \tag{19}$$

The Eq. (19) has the implicit solution

$$\xi = y - \mu\ln|y+\mu| + C, \tag{20}$$

where C is an arbitrary constant, or

$$-\alpha e^{x} = y - \mu\ln|y+\mu| + C. \tag{21}$$

Once the solution $y = y(x)$ is substituted to Eq. (19) in the form

$$t = \int^{x} \frac{dx}{y(x)}, \tag{22}$$

we have the implicit solution $t = t(x)$ for Eq. (18). Upon inversion of this solution we may obtain $q(t)$ and thus have a solution for the original SIR equation.

Initial conditions

The Eq. (13) is a second-order equation while the SIR system of Eq. (1, 2) constitutes a system of two first-order equations with initial conditions $S(0)$ and $I(0)$. It is easy to see that $q(0) = \ln I(0)$ while $\dot{q}(0) = \alpha S(0)$. Thus for Eq. (18) we have the following initial conditions $x(0) = q(0) = \ln I(0)$ and $\dot{x}(0) = \dot{q}(0) - \mu = \alpha S(0) - \mu$. Since both susceptible and infected variables are percentages over the total population, the range of the $q = q(t)$ variable is $(-\infty, 0]$ while $x(t)$ takes similarly values in the same range.

Let us designate for simplicity the values at $t = 0$ of $x(0) = k$ and $\dot{x}(0) = m$; clearly $k = \ln I(0) < 0$ and $m = \alpha S(0) - \mu$. The latter can be either positive, negative or zero, depending on the initial state of the infection and the corresponding infection rate R_0. The defining transformation of Eq. (15) at $t = 0$ becomes $y(k) = m$ and thus the constant C in Eq. (21) is

$$\begin{aligned} C &= -\alpha e^{k} - m + \mu\ln|m+\mu| \\ &\equiv -\alpha I(0) - \alpha S(0) + \mu + \mu\ln|\alpha S(0)|. \end{aligned} \tag{23}$$

In other words, the solution Eq. (21) of the differential equation of Eq. (19) should be solved for $x \geqslant k$ since at $t = 0$ we have $x(0) = k$. Thus, the original SIR problem has solution given by

$$-\alpha e^{x} = y - \mu\ln|y+\mu| - \alpha I(0) - \alpha S(0) + \mu + \mu\ln|\alpha S(0)|, \tag{24}$$

or, in the equivalent form

$$\ln\left[\frac{e^{y}}{|y+\mu|^{\mu}}\right]=-\alpha e^{x}+\alpha I(0)+\alpha S(0)-\mu-\mu\ln|\alpha S(0)|, \tag{25}$$

for $x \geqslant \ln I(0)$ and with the final implicit formula given through the integral of Eq. (22) modified as follows:

$$t=\int_{k}^{x}\frac{dx}{y(x)}\equiv\int_{\ln I(0)}^{\ln I(t)}\frac{dx}{y(x)}. \tag{26}$$

Time-dependent infection rate equation

For the time-dependent infection rate we write Eq. (7) as:

$$\frac{d\alpha}{dt}+f(t)\alpha=g(t)\alpha^{2}, \tag{27}$$

$$f(t)=-\frac{\ddot{q}}{\dot{q}}, \tag{28}$$

$$g(t)=e^{q-\mu t}. \tag{29}$$

The Eq. (27) is a Bernoulli equation [25] that can be turned into a linear first order equation by using the transformation $z(t)=1/\alpha(t)$; we obtain

$$\frac{dz}{dt}-f(t)z+g(t)=0. \tag{30}$$

The general solution thus of Eq. (27) obtained through the solution of Eq. (30) is

$$\frac{1}{\alpha(t)}=C''e^{-F(t)}-e^{-F(t)}\int e^{F(t')}g(t')dt', \tag{31}$$

$$F=-\int f(t')dt', \tag{32}$$

where C'' is an arbitrary constant.

Let us now consider the case where the infected population behaves similar to a Gaussian function [11], keeping however also a linear time-term in the exponent that provides some time asymmetry, *i.e.* take

$$q(t)=\beta t^{2}+\gamma t. \tag{33}$$

Simple algebra leads to

$$q-\mu t=\beta t^{2}+(\gamma-\mu)t, \tag{34}$$

$$f(t)=-\frac{\ddot{q}}{\dot{q}}=-\frac{2\beta}{2\beta t+\gamma}, \tag{35}$$

$$g(t)=e^{q-\mu t}=e^{\beta t^{2}+(\gamma-\mu)t}, \tag{36}$$

$$F=-\int f(t')dt'=\int\frac{2\beta}{2\beta t'+\gamma}dt'=\ln(2\beta t+\gamma), \tag{37}$$

and thus the solution of Eq. (31) becomes

$$\frac{1}{\alpha(t)}=\frac{\alpha(0)\gamma}{2\beta t+\gamma}+\frac{K(t)}{2\beta t+\gamma}, \tag{38}$$

$$\begin{aligned}K(t)&=-\int_{0}^{t}(2\beta t'+\gamma)e^{\beta t'^{2}+(\gamma-\mu)t'}dt'\\&=\left[2\beta-(\gamma-\mu)(\gamma+2\beta t)\right]e^{\beta t^{2}+(\gamma-\mu)t}.\end{aligned} \tag{39}$$

This leads to Eq. (9).

COMPLIANCE WITH ETHICS GUIDELINES

The authors Georgios D. Barmparis and Giorgos P. Tsironis declare that they have no conflict of interest or financial conflicts to disclose. All procedures performed in studies involving animals were in accordance with the ethical standards of the institution or practice at which the studies were conducted, and with the 1964 Helsinki declaration and its later amendments or comparable ethical standards.

OPEN ACCESS

REFERENCES

1. Hufnagel, L., Brockmann, D. and Geisel, T. (2004) Forecast and control of epidemics in a globalized world. Proc. Natl. Acad. Sci. USA, 101, 15124−15129
2. Baker, R. E., Yang, W., Vecchi, G. A., Metcalf, C. J. E. and Grenfell, B. T. (2020) Susceptible supply limits the role of climate in the early SARS-CoV-2 pandemic. Science, 369, 315−319
3. Qiu, Y., Chen, X. and Shi, W. (2020) Impacts of social and economic factors on the transmission of coronavirus disease 2019 (COVID-19) in China. J. Popul. Econ., 33, 1−46
4. Ardabili, S. F., Mosavi, A., Ghamisi, P., Ferdinand, F., Varkonyi-Koczy, A. R., Reuter, U., Rabczuk, T. and Atkinson, P. M. (2020) COVID-19 outbreak prediction with machine learning. Algorithms, 13, 249
5. Ardabili, S., Mosavi, A., Band, S. S. and Varkonyi-Koczy, A. R. (2020) Coronavirus disease (COVID-19) global prediction using hybrid artificial intelligence method of ANN trained with grey wolf optimizer. In: 2020 IEEE 3rd International Conference and Workshop in Óbuda on Electrical and Power Engineering (CANDO-EPE), pp. 000251–000254
6. Pinter, G., Felde, I., Mosavi, A., Ghamisi, P. and Gloaguen, R.

(2020) COVID-19 pandemic prediction for hungary; a hybrid machine learning approach. Mathematics, 8, 890
7. da Silva, R. G., Ribeiro, M. H. D. M., Mariani, V. C. and Coelho, L. D. S. (2020) Forecasting Brazilian and American COVID-19 cases based on artificial intelligence coupled with climatic exogenous variables. Chaos Solitons Fractals, 139, 110027
8. Zhao, S. and Chen, H. (2020) Modeling the epidemic dynamics and control of COVID-19 outbreak in China. Quant. Biol., 8, 11−19
9. Albani, V. V. L., Velho, R. M. and Zubelli, J. P. (2021) Estimating, monitoring, and forecasting the COVID-19 epidemics: A spatiotemporal approach applied to NYC data. Sci. Rep., 11, 9089
10. Lytras, T., Panagiotakopoulos, G. and Tsiodras, S. (2020) Estimating the ascertainment rate of SARS-COV-2 infection in Wuhan, China: implications for management of the global outbreak. medRxiv, doi: 10.1101/2020.03.24.20042218
11. Barmparis, G. D. and Tsironis, G. P. (2020) Estimating the infection horizon of COVID-19 in eight countries with a data-driven approach. Chaos Solitons Fractals, 135, 109842
12. Kermack, W. O. and McKendrick, A. G. (1927) A contribution to the mathematical theory of epidemics. Proc. R. Soc. Lond., A Contain. Pap. Math. Phys. Character, 115, 700−721
13. Abadi, M. Agarwal, A., Barham, P., Brevdo, E., Chen, Z., Citro, C., Corrado, G. S., Davis, A., Dean, J., Devin, M., *et al.* (2015) TensorFlow: Large-scale machine learning on heterogeneous systems. arXiv, 1603.04467
14. Keras. https://keras.io, Accessed: April 1, 2021
15. Kingma, D. and Ba, J. (2017) Adam: a method for stochastic optimization. arXiv, 1412.6980
16. Roser, M., Ritchie, H., Ortiz-Ospina, E. and Hasell, J. (2020) Coronavirus pandemic (COVID-19). https://ourworldindata.org/coronavirus, Accessed: April 1, 2021
17. The code. https://github.com/georgiosdb/PINN-COVID-19, Accessed: April 1, 2021
18. Raissi, M., Perdikaris, P. and Karniadakis, G. E. (2019) Physics-informed neural networks: A deep learning framework for solving forward and inverse problems involving nonlinear partial differential equations. J. Comput. Phys., 378, 686−707
19. Hunter, J. D. (2007) Matplotlib: A 2D graphics environment. Comput. Sci. Eng., 9, 90−95
20. Matplotlib basemap toolkit. https://matplotlib.org/basemap, Accessed: April 1, 2021
21. Rosakis, P. and Marketou, M. E. (2020) Rethinking case fatality ratios for COVID-19 from a data-driven viewpoint. J. Infect., 81, e162−e164
22. Kaxiras, E., Neofotistos, G. and Angelaki, E. (2020) The first 100 days: Modeling the evolution of the COVID-19 pandemic. Chaos Solitons Fractals, 138, 110114
23. Schüttler, J., Schlickeiser, R., Schlickeiser, F. and Kröger, M. (2020) COVID-19 predictions using a Gauss model, based on data from April 2. Physics, 2, 197−212
24. Asteris, P. G., Douvika, M. G., Karamani, C. A., Skentou, A. D., Chlichlia, K., Cavaleri, L., Daras, T., Armaghani, D. J. and Zaoutis, T. E. (2020) A novel heuristic algorithm for the modeling and risk assessment of the COVID-19 pandemic phenomenon. Comput. Model. Eng. Sci., 125, 815−828
25. Polyanin, A. D. and Zaitsev, V. F. (2002) Handbook of Exact Solutions of Ordinary Differential Equations, 2nd Ed., New York: Chapmand and Hall/CRC

